Available online at www.sciencedirect.com
SCIENCE DIRECT
Polymer 46 (2005) 9005–9014
polymer
www.elsevier.com/locate/polymer

Effect of hydrodynamics on dynamics of phase separation in polystyrene/poly(vinyl methyl ether) blend

K. El Mabrouk, M. Bousmina*

Canada Research Chair on Polymer Physics and Nanomaterials, Department of Chemical Engineering, CREPEC, Laval University, Que., Canada G1K 7P4

Received 5 January 2005; received in revised form 4 July 2005; accepted 7 July 2005
Available online 10 August 2005

Abstract

Polystyrene/poly(vinyl methyl ether) (PS/PVME) phase diagram was assessed by rheological tools and by on-line microscopy observations both under quiescent and shear flow conditions. Shear flow was found to induce both mixing and demixing of the mixture depending on the amplitude of the imposed shear rate. Viscoelastic properties of PS/PVME blends were also measured under steady shear flow near the phase separation temperature. At lower shear rate, flow enhances concentration fluctuation and induces phase segregation. At high shear rate, flow suppresses fluctuations and the polymer mixture keeps its miscible state. Several rheological signatures of phase transition were found. In steady shear flow, a secondary plateau in viscosity was observed when the temperature was close to T_s whereas, at the start-up shear flow, transient shear stress showed a second overshoot after a few minutes of shearing.

Keywords: Polymer blends; Shear-induced phase changes; Flow fields

1. Introduction

Phase segregation in polymer blends is a non-trivial problem that involves complex combinations of thermodynamics and kinetics. Under quiescent conditions, phase segregation or phase homogenization may be induced by variation in temperature, pressure, and concentration. When flow comes in play, the phase dynamics becomes even more complex and stress, strain and rate of strain of the imposed flow field become of importance. Therefore, the description of phase diagram under flow needs non-trivial coupling between flow, thermodynamics and eventually with kinetics.

The literature is very rich with respect to the phase behavior of phase segregating polymer blends under quiescent conditions. However, only few data are available regarding phase segregation under flow field. Flow such as shear may induce mixing or demixing depending on the flow conditions. Mani et al. [1], carried out step-rate experiments in homogeneous PS/PVME blends and observed a second overshoot in both shear stress and first normal stress difference, a fact that was related to the occurrence of shear induced demixing (SID). This was confirmed by simultaneous fluorescence measurements. Fernandez et al. [2], Hindawi et al. [3], and Madbouly et al. [4], have observed both shear induced mixing (SIM) and demixing in PS/PVME blends depending on the magnitude of shear rate. Chen et al. [5] and Remediakis et al. [6] carried out rheo-optical experiments and pointed out the role of hydrodynamic instabilities in the flow-induced patterns. Kim et al. [7] and Hashimoto et al. [8] inferred the SIM behaviour for PS and polybutadiene blend to the continuous deformation and breakup mechanisms of the dispersed droplets. In spite of the various studies, the effect of flow on phase diagram is still poorly understood and only a few experimental results are available in this field. From theoretical point of view there are some important efforts, but the theory is still incomplete.

The main objective of this work is to report on the effect of flow on the phase diagram of PS/PVME blend. The phase diagram of such a blend is of lower critical solution temperature (LCST) type as was primarily assessed by various techniques. Phase segregation under flow field was evaluated by on-line optical microscopy and on-line light transmission during shearing. Various flow histories

* Corresponding author. Fax: +1 418 656 5993.
E-mail address: bousmina@gch.ulaval.ca (M. Bousmina).

0032-3861/$ - see front matter © 2005 Elsevier Ltd. All rights reserved.
doi:10.1016/j.polymer.2005.07.021

involving steady and transient shear tests were used to assess the morphological changes at various temperatures and shear rates.

2. Materials and methods

Polystyrene (PS) was purchased from Polymer Source Inc. and had $M_w = 104{,}000$ and a polydispersity index (PI) of 1.05. Poly(vinyl methyl ether) (PVME) was obtained from scientific polymer products and had $M_w = 90{,}700$ and a PI of 1.95. M_w and PI of PS were determined by size exclusion chromatography (SEC) equipped with UV and refractive Viscotek triple detector, while M_w and PI of PVME were determined by gel permeation chromatography and by light scattering.

PS/PVME blends with compositions 90/10, 75/25, 50/50, 25/75, and 10/90 were prepared by continuous mechanical mixing of the components in toluene. The solvent was evaporated by exposure to air at room temperature during 3 days. The samples were then slowly dried under vacuum at 70 °C for at least 2 weeks to remove eventual traces of moisture and toluene.

The effect of flow on the phase diagram was examined by two methods. The first one consists in using an on-line optical microscope (Axioplan, Zeiss Co.) coupled with a shearing hot plate from Linkam Scientific Instruments Ltd (model CSS 450). A schematic illustration of the shearing device is shown in Fig. 1. The sample was placed between two windows that are in close thermal contact with silver heaters. The bottom window, located within the lower section of the shearing cell, is attached to a metal carrier that can rotate under the control of a stepper motor. This allows imposition of constant shear rate to the sample under observation. Cloud point was taken as the temperature at which the first sign of cloudiness appears. The second method consists in using rheo-optics of the ARES-LS constant strain rheometer from rheometrics. A sample of 38 mm in diameter and 0.5 mm in thickness was placed between the two parallel plates of the rheometer. During shearing, on-line light transmission was monitored at various temperatures in molten state. Three types of measurements were carried out:

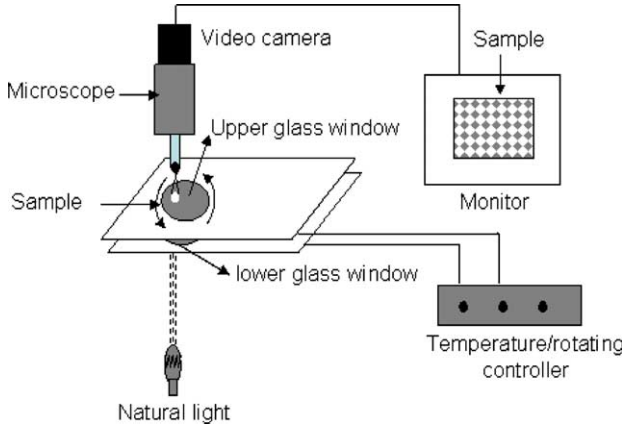

Fig. 1. Schematic representation of the shear flow apparatus coupled with microscope used in this works.

1. Three steps regime: (i) First a frequency sweep was performed under small amplitude oscillatory shear flow (SAOS) at 5 °C below the critical temperature of phase segregation, T_c, (ii) the sample was then subjected to steady shear flow at 1, 2, 3 and 5 s^{-1} during 1000 s and then (iii) the steady flow was stopped and frequency sweep was carried again under SAOS conditions.
2. Start-up shear flow at 1, 2, 3, and 5 s^{-1} in the homogeneous region at 5 °C below T_c.
3. Steady shear flow measurement in a wide temperature range from the homogeneous to the two phase regime. Steady shear viscosity and first normal stress difference were measured in shear rate interval ranging between 10^{-2} and 8 s^{-1}.

3. Results and discussion

3.1. Phase diagram under shear flow

Phase diagram of PS/PVME blend was constructed from data collected by on-line optical microscopy and rheological measurements. Dynamic temperature sweep experiments were used to determine the phase-separation temperature for various blend compositions. The results are reported in Fig. 2. The first deviation of G' as a function of temperature was taken as the binodal temperature [9]. These results were compared with the cloud points obtained by optical observations. The phase diagram in the absence of flow obtained with both methods is presented in Fig. 3. To examine the effect of flow in steady shear on the phase diagram of the blend, the samples were placed in the cell of the Linkam shearing device and heated at about 110 °C. The samples were then sheared at constant shear rate, while the temperature was increased to higher values at a rate of 2 °C min^{-1}. The texture of the sample was recorded by a CCD camera mounted directly on the microscope (Fig. 1). Shear rate was varied in the range of 0–24 s^{-1} and the cloud point was determined by observing the turbidity of the samples. Fig. 4 shows the effect of shear rate on the cloud point for various blend compositions. Depending on the magnitude of the applied shear rate, three regions can be distinguished. At low shear rate, the cloud point decreases gradually, reaches a minimum, and then increases before reaching at high shear rates a steady state value. The location of the minimum does not depend on the composition, whereas the magnitude of the plateau at high shear rate does. The effect of shear on the phase diagram was also examined by light transmission. A sample of about 0.5 mm in thickness and 38 mm in diameter was placed

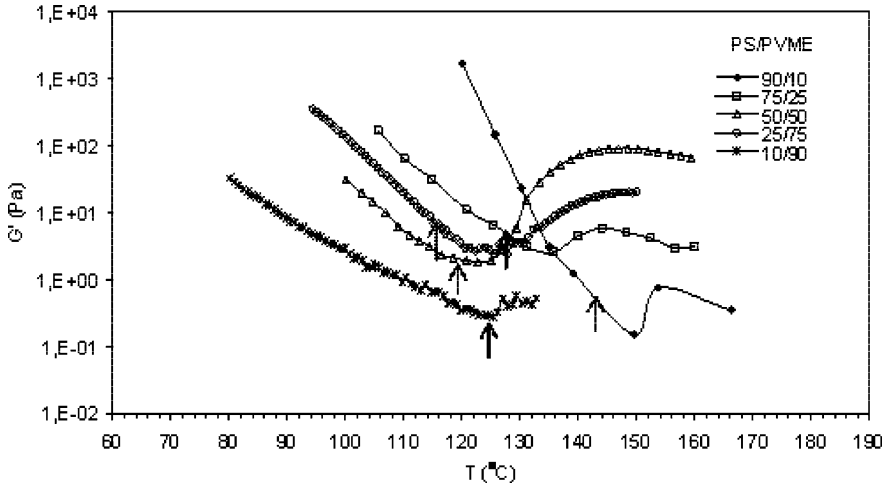

Fig. 2. Typical dynamic temperature ramps of storage modulus G' for the PS/PVME blend at different compositions, frequency $\omega = 0.013$–0.3 rad s^{-1} and strain amplitude 3–7%. The ↑ indicates the rheologically determined phase separation temperature (binodal) from the intersection of the tow of slopes 1 and 2, as the blend is heated with the rate of 0.5 °C min^{-1}.

between two quartz parallel plates of the rheometer. Collimated laser light with a wavelength of 670 nm was emitted from the laser diode on top of the sample. The transmitted light intensity passing through the sample was measured under shear flow at a given shear rate. To make comparison between the two techniques, the rate of heating was kept the same (2 °C min^{-1}). Fig. 5 shows the critical temperature under shear flow for the composition PS/PVME 10/90 obtained by Linkam shearing devise and laser light transmission. In spite of the small differences between the values, the behaviour remains the same. The results obtained by the two techniques show that PS/PVME blend presents both SIM and SID behaviors. The laser light transmission experiments were limited to mixtures with low concentration of PS phase and to maximum shear rate of 8 s^{-1}. Higher shear rates induce secondary flow effects.

To better visualise the effect of shear rate on phase diagram, the cloud point is reported as a function of PS weight fraction for various shear rates (Fig. 6). The figure reports also the cloud point under quiescent conditions (dashed line). Clearly, for blends with PS-rich phase, small values of shear rate shift the phase diagram at lower temperatures (SID), whereas at shear rates larger than a certain critical shear rate, $\dot{\gamma}_c$, the shear has an opposite effect shifting the phase diagram at higher values (SIM). To accurately determine $\dot{\gamma}_c$, the normalised factor, D, was

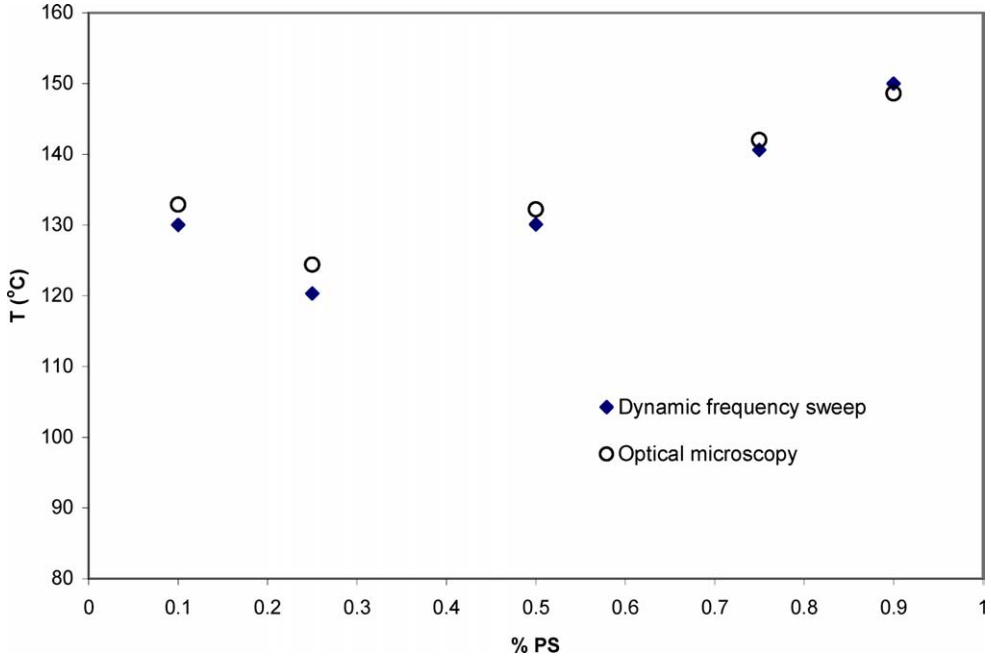

Fig. 3. Phase diagram for the PS/PVME blend obtained from optical microscopy observation and rheology.

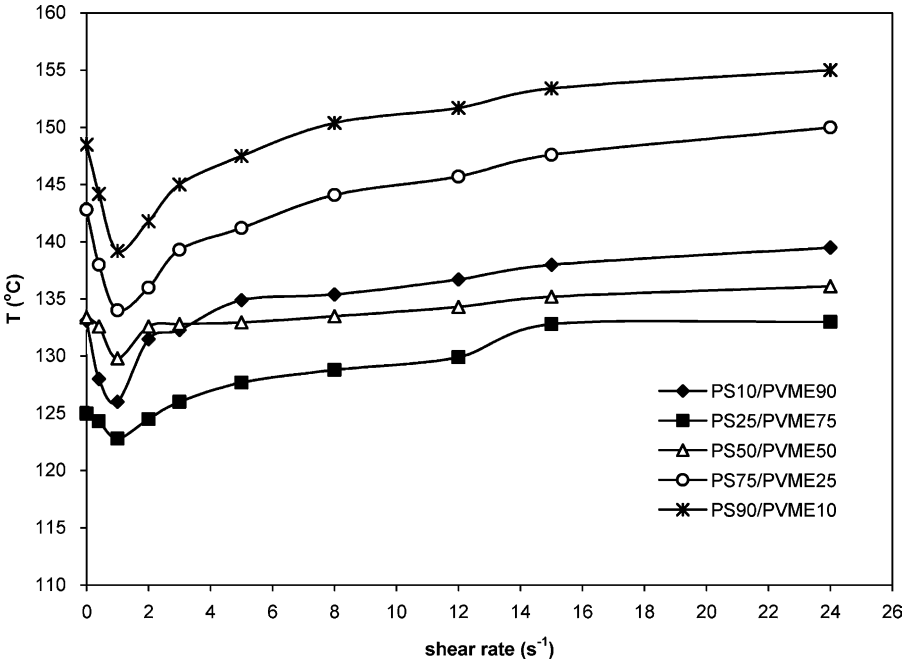

Fig. 4. Shear rate dependence of cloud points for different composition ratios of PS/PVME.

plotted as a function of shear rate. D is given by:

$$D = \frac{T_c(\dot{\gamma}) - T_c(0)}{T_c(0)} \quad (1)$$

Where $T_c(\dot{\gamma})$ is the value of T_c in the presence of shear and $T_c(0)$ is the critical temperature under quiescent conditions. Fig. 7 presents the normalised factor D as a function of $\dot{\gamma}$ for various blend's compositions. When D is negative, the behavior is of SID type, whereas positive values of D imply a process proceeding through SIM mechanism. Empirically, the experimental results for the variation of the D ratio as a function of shear rate were found to be well described by a logarithmic curve fit:

$$D = \ln(s_1 \dot{\gamma}^{s_2}) \quad (2)$$

The computed values of S_1 and S_2 for the various PS/PVME compositions are given in Table 1. The critical shear rate, $\dot{\gamma}_c$, is then determined from Fig. 7. It was taken as the value of shear rate, where the D curve intersects the horizontal line 0. The variation of $\dot{\gamma}_c$ with composition is shown in Fig. 8. Clearly, $\dot{\gamma}_c$ is constant both in PS and in PVME rich phases and takes some average value for intermediate composition.

To explain the effect of shear on phase diagram, Wolf [10] used an argument based on the loss of entropy due to the chains deformation during flow. Analytically this comes to assume an additional free energy stored during flow [11–13]:

$$\frac{\partial^2 \Delta G(\dot{\gamma})}{\partial \varphi^2} = \frac{\partial^2 \Delta G_{eq}}{\partial \varphi^2} + \frac{\partial^2 \Delta E_s}{\partial \varphi^2} \quad (3)$$

Where $\Delta G(\dot{\gamma})$ is the total free energy in the presence of flow and ΔG_{eq} is the free energy under quiescent conditions. When the term $\partial^2 \Delta E_s / \partial \phi^2$ is positive, shear will enhance miscibility (SIM) and when $\partial^2 \Delta E_s / \partial \phi^2$ is negative, shear-induces rather demixing (SID). Many authors used such argument and related the additional stored energy to the

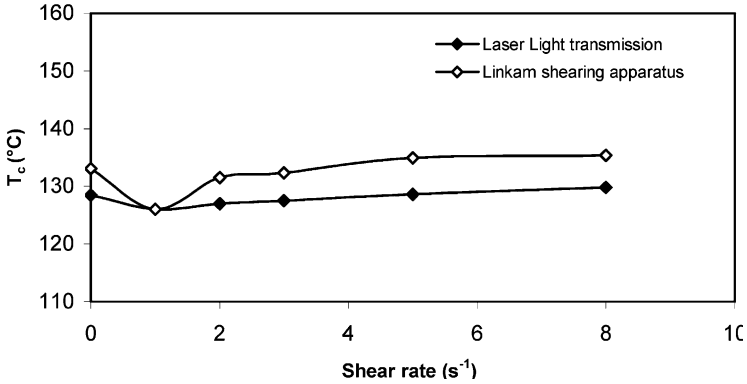

Fig. 5. Shear rate dependence of cloud points for PS/PVME 10/90 obtained by optical observation and laser light transmission at different shear rates.

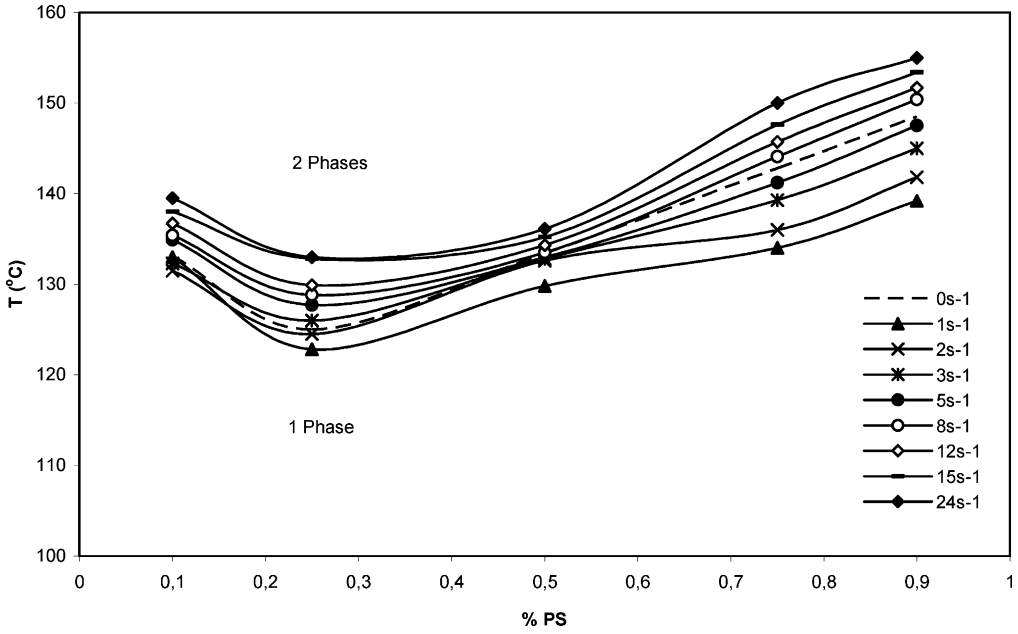

Fig. 6. Phase diagram of PS/PVME under the effect of different shear rate.

shear stress or first normal stress difference (which is a function of chains deformation). However, such classical thermodynamics argument is only valid under equilibrium or at least in the quasi-equilibrium state. Clearly, the time factor is absent from such analysis. When the binary mixture is sheared close to the critical point, there are at least two time factors that govern the evolution of the process during flow: The time scale related to flow $\dot{\gamma}^{-1}$, and the characteristic lifetime, τ, of the critical fluctuations. The effect of flow on phase diagram will then depend on the product $\dot{\gamma}\tau$. Two regimes are possible: $\dot{\gamma}\tau > 1$ strong-shear regime and $\dot{\gamma}\tau < 1$ weak-shear regime. It comes then that the pertinent parameter is not the stored energy but the rate of its storage or the time within which this energy is being stored by the mixture. When the flux of energy brought to the mixture is small (low shear rate), the local deformation of chains enhances the amplitude of fluctuations and drive the mixture into two-phase system (SID). Whereas under strong flow (high shear rate), the chains that are largely deformed due to flow do not participate to the concentration

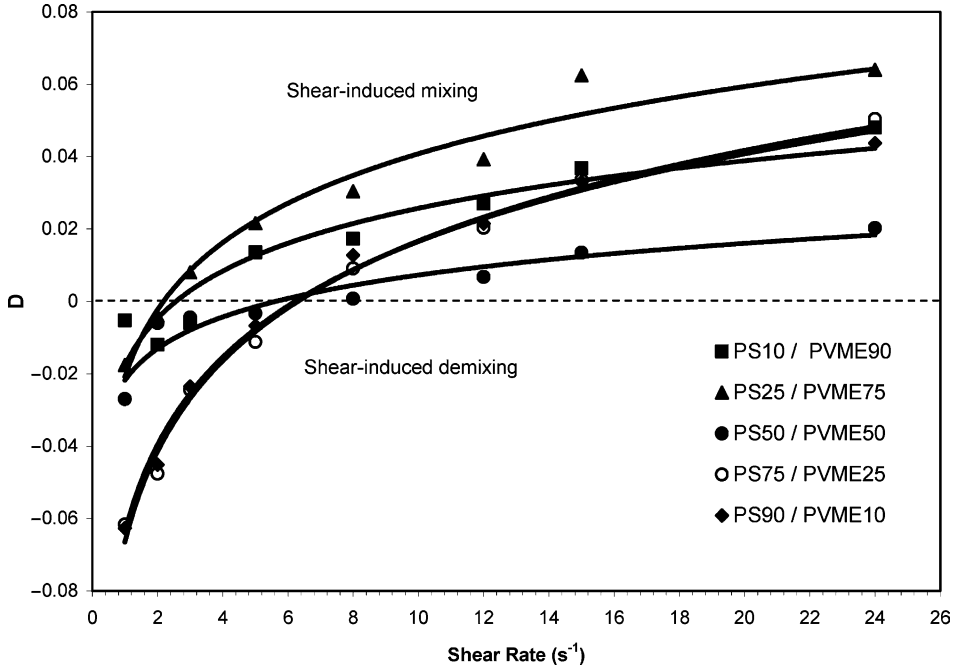

Fig. 7. *D* versus shear-rate curve for PS/PVME blends.

Table 1
Determination of s_1 and s_2 value for different PS/PVME compositions

Polymer blend	s_1	s_2
PS90/PVME10	0.9373	0.0349
PS75/PVME25	0.9357	0.0361
PS50/PVME50	0.9784	0.0126
PS25/PVME75	0.9793	0.0268
PS10/PVME90	0.9823	0.0189

fluctuation. Therefore, small fluctuations are suppressed and the system goes back to the equilibrium homogeneous state (SIM). Such a time-dependent process depends on how $\dot{\gamma}^{-1}$ compares to τ. The critical shear rate $\dot{\gamma}_c$ equals then $1/\tau$. τ may be thought of here as the time of disentanglement in the Rouse sense. Rouse time is given by:

$$\tau_{\text{Rouse}} = \frac{\varsigma N^2 b^2}{3\pi^2 k_B T} \tag{4}$$

With K_B the Boltzmann constant, T, the absolute temperature, ς the friction coefficient, b the statistical segment length and N the degree of polymerisation. The following equations were used to calculate the Rouse time:

$$\varsigma = \varphi_i \frac{N_i}{N_e} \varsigma_0 \tag{5}$$

Where N_i is the degree of polymerisation of the dispersed phase M_{wd}/M_{0d}, $N_e = M_e/M_0$ and ς_0 is given by:

$$\varsigma_0 = (\varphi_{PS}\varsigma_{0(PS)}^{1/2} + \varphi_{PVME}\varsigma_{0(PVME)}^{1/2})^2 \tag{6}$$

$\varsigma_{0(PS)}$ and ς_{0PVME} are expressed by

$$\varsigma_{0(PS)} = \frac{48}{5}\frac{V(N_{e(PS)})^2}{b_{PS}^2 N_{PS}^3}\eta_{PS} \text{ and}$$
$$\varsigma_{0(PVME)} = \frac{48}{5}\frac{V(N_{e(PVME)})^2}{b_{PVME}^2 N_{PVME}^3}\eta_{PVME} \tag{7}$$

The total molar volume, V, is equal to $V=(V_{PS}V_{PVME})^{1/3}$ and the number N in Eq. (4) is given by:

$$N = \left(\varphi_{PS}N_{(PS)}^{1/2} + \varphi_{PVME}N_{(PVME)}^{1/2}\right)^2 \tag{8}$$

M_e is determined from the plateau modulus in G':

$$M_{e(i)} = \frac{\rho RT}{G_{N0(i)}} \tag{9}$$

At a first approximation, the following Rouse time of the mixture may be considered as a mean value of the Rouse times of the individual components. That is to say that the dynamics of disentanglement is dominated by the component with the longest Rouse time. Calculated Rouse times are given in Table 2. The results clearly show that the critical shear rate, $\dot{\gamma}_c$, separating SIM and SID regimes is of order of the inverse of the average Rouse time of the mixture. From microscopic viewpoint, this time may be also seen as the time required for the amplitude of fluctuations to reach a portion of the amplitude corresponding to the critical wavelength, λ_c, of phase separation as predicted by Cahn–Hilliard theory. This amplitude depends of course on concentration. The critical time τ is then given by:

$$\tau = \frac{6\pi\eta\xi(\varphi)^3}{k_B T} \tag{10}$$

With η the viscosity of the blend and ξ the correlation length of fluctuations. Our experimental results show that $\xi(\phi)$ is a decreasing function of PS weight fraction (Fig. 9). For PS rich phase, the ratio of about 100, whereas for PVME rich phase, the ratio is of about 10. This is qualitatively coherent with the difference in magnitude between the disentanglement times of PS and PVME.

In Fig. 10 an empirical equation was proposed for the variation of D as a function of shear rate. In terms of polynomial form, D varies almost as $\dot{\gamma}^{0.67}$ (Fig. 10). This is consistent with the Johany and Leibler theory [14] that expresses the interfacial tension near the critical point as

$$\alpha = \frac{2}{3}\frac{k_B T}{b^2 N^{1/2}} D^{3/2} \tag{11}$$

The equilibrium of the system is given by equality of viscous stresses and interfacial stresses. This leads to the expression of D as a function of $\dot{\gamma}$:

$$D = \left(\frac{1}{4}\frac{Nb^3}{k_B T}\right)^{2/3} \dot{\gamma}^{2/3} \propto \dot{\gamma}^{0.66} \tag{12}$$

The experimental exponent agrees fairly well with the

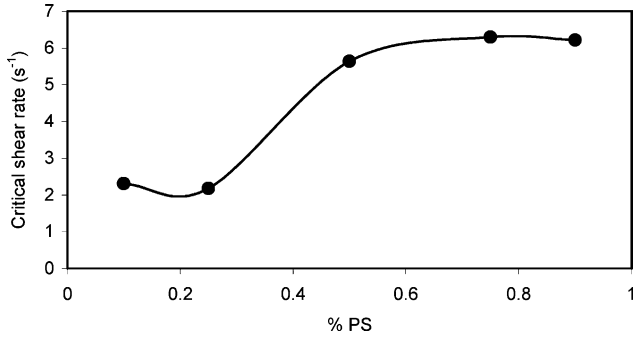

Fig. 8. Critical shear rate as a function of PS volume fraction.

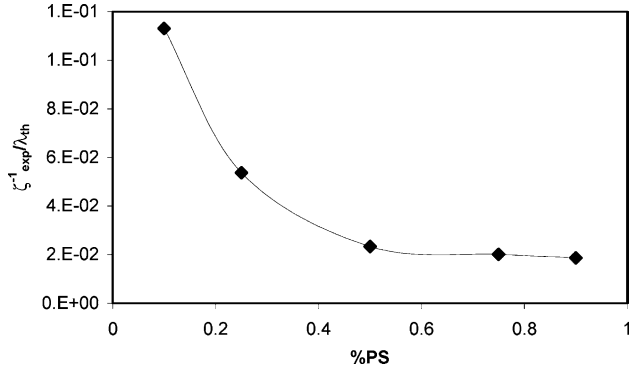

Fig. 9. $\xi_{exp}^{-1}/\lambda_{th}$ as a function of PS volume fraction.

Table 2
Experimental and theoretical of Rouse time

%PS	$\dot{\gamma}_c(s^{-1})$	τ_c (s)	T_c (°C)	η (Pa-s)	$\dot{\gamma}_{c(\text{Rouse})}(s^{-1})$	$\tau_{c(\text{Rouse})}$ (s)	ς (J s m^{-2})
0.1	2.31	0.432	133.1	110.786	1.95	0.514	0.280×10^{-4}
0.25	2.18	0.458	125.0	356.155	2.21	0.453	1.112×10^{-4}
0.5	5.64	0.177	133.4	1115.223	2.22	0.451	2.578×10^{-4}
0.75	6.30	0.158	142.8	2432.287	4.94	0.203	1.312×10^{-4}
0.9	6.22	0.160	148.5	9509.341	5.45	0.183	1.205×10^{-4}

theoretical value. In the case of liquid binary mixtures (or small molecular weight components), the correlation length ξ is given by: $\xi=\xi_0 D^{-\nu}$, with ξ_0 is an amplitude and ν takes a universal value of 0.63 [15]. Inserting the expression ξ in Eq. (10), the crossover reduced temperature writes then:

$$D=\left(\frac{6\pi\eta\xi_0^3}{k_B T}\right)^{1/3\nu}\dot{\gamma}^{1/3\nu}\propto\dot{\gamma}^{0.54} \tag{13}$$

The exponent resulting from binary liquid mixtures is slightly smaller than that of polymer mixtures.

3.2. Morphology evolution under shear flow

To assess the morphology evolution under flow field, real time images were recorded during heating at a shear rate of 2 °C min^{-1} during shearing. The typical morphologies are shown in Fig. 11. At zero shear rate and at 120 °C, PS/PVME 25/75 remains miscible. When the temperature reaches 125 °C, the mixture becomes turbid and phase segregation takes place. Under shear flow at $\dot{\gamma}=1$ s^{-1}, the flow-enhances concentration fluctuations and small droplets appear in the mixture. Such droplets grow progressively in time and depending on the intensity of shear, they undergo a more or less important deformation in the direction of flow. This can be clearly seen in Fig. 11, where long and thin parallel filaments develop in the direction of flow rendering the mixture more opaque. Under large shear rates, the stretching ratio is very high and the filaments break-up under the combination of flow and Rayleigh instabilities re-establishes the one phase equilibrium state (SIM). The critical temperature of phase separation under shear flow at

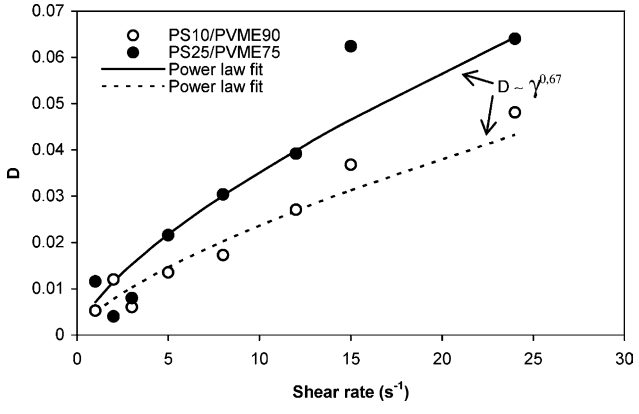

Fig. 10. Experimental and power law fit of D as a function of shear rate.

$\dot{\gamma}=1$ s^{-1} was found to be around 122.8 °C. When shear rate reaches $\dot{\gamma}=5$ s^{-1}, the turbidity of the sample changes gradually in time to restore after few minutes the miscible state. These results agree well with the results presented previously in Fig. 4. High shear rates have a tendency to shift the segregation temperature, T_c, to higher values (SIM), while low shear rates shift T_c to lower values (SID).

3.3. Effect of shear history on the morphology

3.3.1. Start-up experiments

It was evidenced in the previous section that the critical temperature of phase separation decreases with shear rate and then increases gradually to reach a constant value at high shear rate. It was also observed that high shear rates tend to suppress the concentration fluctuations driving the blend towards equilibrium miscibility. The previous experiments were carried under continuous heating at constant shear rate and heating rate (2 °C min^{-1}). Let us now examine the phase behavior under transient regime involving time effects. For this purpose, a blend of composition 25/75 was maintained at a temperature 5 °C lower than the critical temperature (homogeneous region) and then submitted to start-up flow at constant shear rate. Fig. 12 shows the measured transient shear stress as a function of time at various applied shear rates (1, 2, 3 and 5 s^{-1}). Fig. 12(a) corresponding to a shear rate of 1 s^{-1} exhibits a slight overshoot after few seconds of shearing. This is similar to the classical viscoelastic overshoot usually seen in start-up flow of non-dilute polymer solutions due stretching and rotation of polymer chains (as can be confirmed by birefringence experiments). After about 350 s, the shear stress starts to increase in function time and then reaches a steady state value [16,17]. Light transmission experiments revealed a net decrease in the transmitted intensity indicating the occurrence of phase separation. When shear rate is increased to 2 s^{-1}, a second overshoot in shear stress appears a few minutes after the onset of shearing. Such a second overshoot is a fingerprint of an additional elasticity due to the creation of an interface separating the blend's component domains. The same result is observed at shear rate of 3 s^{-1}. When shear rate reaches 5 s^{-1}, only one overshoot in the shear stress is observed confirming the results about SIM observed in the previous section.

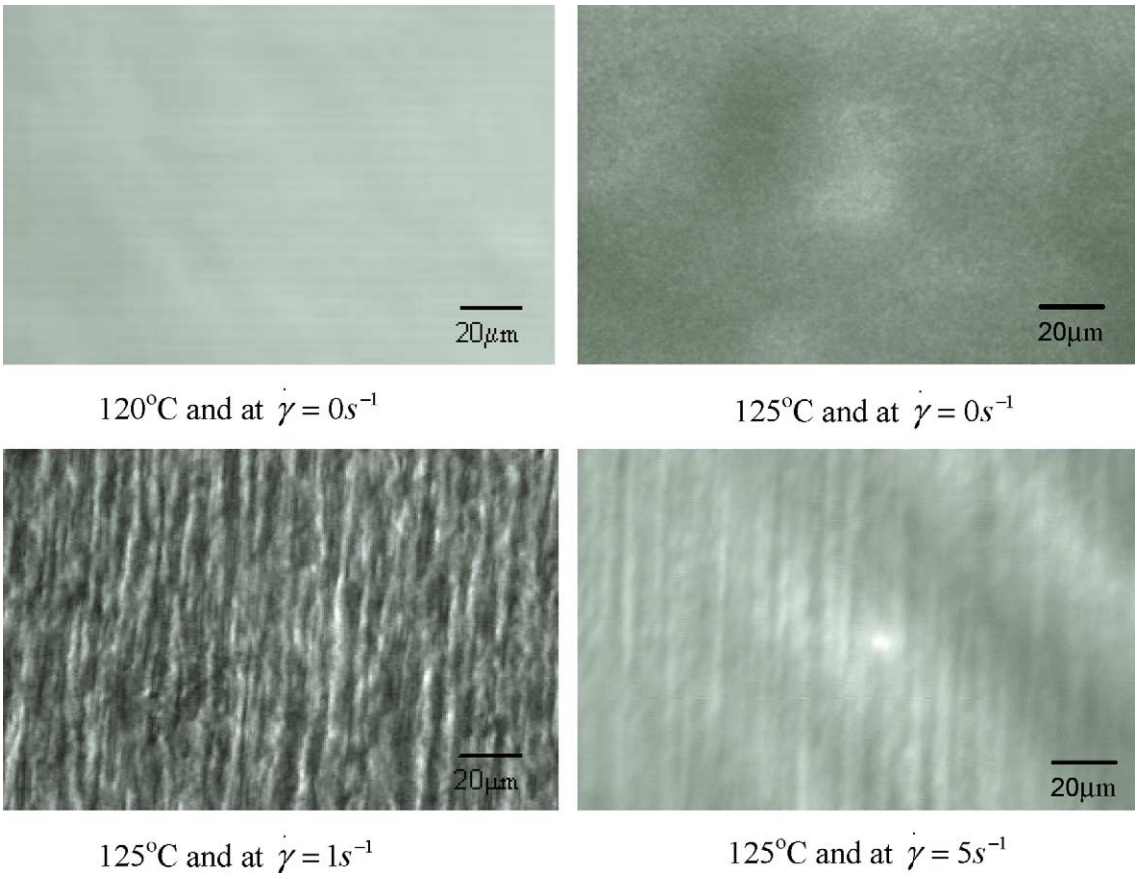

Fig. 11. Optical micrographs obtained from phase contrast microscopy for PS25/PVME75 at different shear rates and at different temperatures.

3.3.2. Preshear effect on phase separation

To examine the preshear effect on morphology change, experiments were carried out at 5 °C below the temperature of phase separation for the blend PS/PVME 25/75. First the blend was submitted to an isothermal dynamic frequency sweep. A second dynamic frequency sweep was applied at the same temperature but after a preshear at 0, 1, 2, 3 and 5 s^{-1} during 1000 s. This time ensures steady state regime as was evidenced by transient experiments in the previous section. The results are summarized in Fig. 13. Before shearing, G' does not show any shoulder at lower frequencies and the slop of $\log(G')$ as a function of $\log \omega$ is around 2, (typical of homogenous systems). After preshearing at 1, 2 and 3 s^{-1} during 1000 s, a shoulder in G' appears in the low-frequency region indicating the presence of a two phase system. Such a shoulder disappears when the preshear was performed at 5 s^{-1}. This confirms once again the previous observations about the critical shear rate that separates SIM and SID processes.

3.3.3. Steady shear flow

In steady shear, both viscosity and first normal stress difference were measured using cone and plate geometry. PS/PVME 25/75 was chosen as a model blend for these experiments because the PS rich blend limits the use of cone-plate setup at low temperatures. The time of shearing at each shear rate was 1000 s, long enough to ensure steady shear conditions as was previously verified by transient measurements in shear rate start-up flow.

Under quiescent conditions, the blend phase separates at 125 °C. Fig. 14 shows the shear viscosity and the first normal stress difference data at three temperatures 100, 110 and 125 °C. For the two first temperatures, the viscosity of the blend shows a Newtonian plateau at low shear rate. The results of the previous sections have shown that at a temperature lower than 125 °C, the mixture remains miscible. At this stage, we might conclude that the mixture is miscible and this can be confirmed by the examination of the first normal stress difference that varies almost as $\dot{\gamma}^2$, which is typical for homogeneous systems. When the temperature reaches 125 °C, the results show a clear transition to a second plateau at high shear rates. The first plateau is related to an immiscible morphology at low shear rates ($\dot{\gamma} \leq 2\ s^{-1}$). This could be confirmed by the increase in the value of the first normal stress difference (slop of N_1 is <2) due to the presence of an interface in the polymer mixture. When shear rate exceeds 2 s^{-1}, the system begins to restore its miscible state characterized by the second plateau in viscosity at high shear rates. The critical shear rate separating these two regimes (about $\dot{\gamma}_c \cong 2\ s^{-1}$)

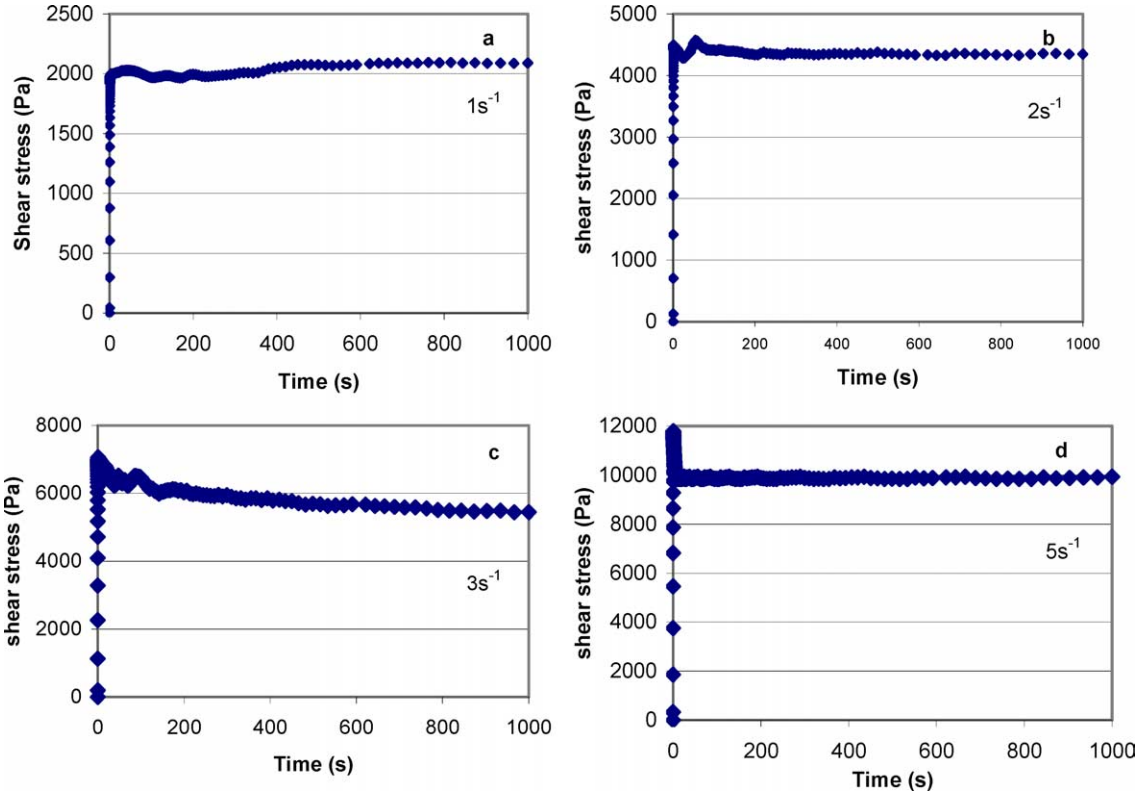

Fig. 12. Time dependence of shear stress of PS/PVME 25/75 at various shear rates and at 123 °C.

coincides very well with the value of $\dot{\gamma}_c$ determined previously from Fig. 7.

4. Concluding remarks

In this work, we have shown through various flow histories how hydrodynamics affects the dynamics of phase separation in PS/PVME blend. Two regimes were found corresponding to: $\dot{\gamma}\tau > 1$ strong-shear regime and $\dot{\gamma}\tau < 1$ weak-shear regime. Experimental results revealed that the two regimes are characterised by a shear induced mixing (SIM) and shear induced demixing (SID), respectively. The time scale separating these two regimes was found to be of the order of magnitude of Rouse time.

The normalised shift in temperature, D, was found to vary proportionally to $\dot{\gamma}^{0.67}$, in agreement with the theoretical predictions.

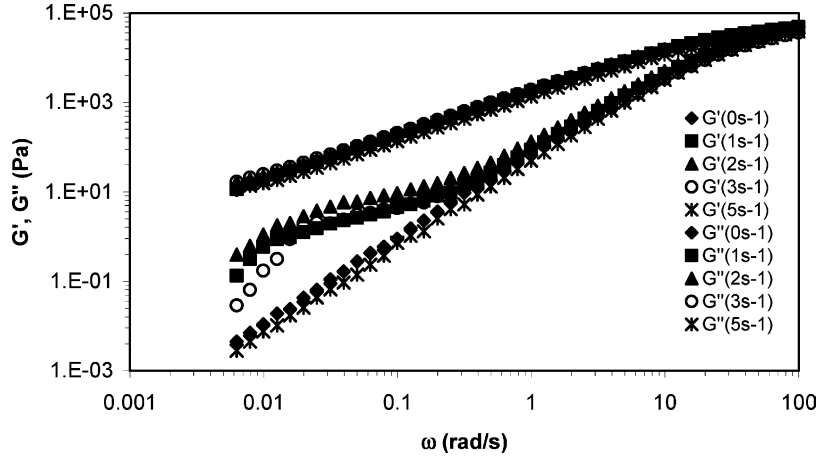

Fig. 13. Dynamic moduli of PS25/PVME75 at 123 °C before and after shearing during 1000 s.

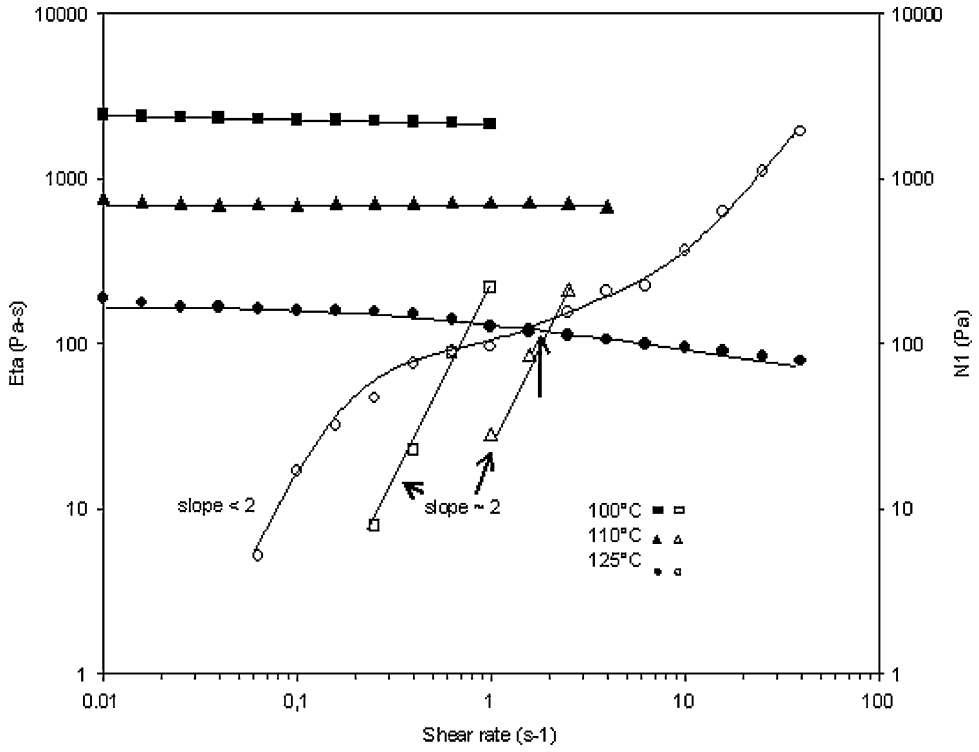

Fig. 14. Steady shear viscosities and first normal stress different of PS25/PVME75 blend at different temperatures.

To the best of our knowledge, this is the first time that the same blend has been fully characterised using various techniques under both quiescent conditions and under flow. Flow effect was examined both in steady and transient regimes.

Acknowledgements

This work was financially supported by the NSERC (Natural Sciences and Engineering Research Council of Canada), Canada Research Chair on Polymer Physics and Nanomaterials and the Steacie fellowship grants.

References

[1] Mani M, Malone MF, Winter HH. Macromolecules 1992;25:5671.
[2] Fernandez ML, Higgens JS, Horst R, Wolf BA. Polymer 1995;36:149.
[3] Hindawi A, Higgens JS, Weiss RA. Polymer 1992;33:2522.
[4] Madbouly S, Ohmomo M, Ougizawa T, Inoue T. Polymer 1999;40:1465.
[5] Chen ZJ, Wu RJ, Shaw MT, Weiss RA, Fernandez ML, Higgins JS. Polym Eng Sci 1995;35:2.
[6] Remediakis NG, Weis RA, Shaw MT. Rubber Chem Technol 1997;70:1.
[7] Kim S, Hobbie EK, Yu JW, Han CC. Macromolecules 1997;30:8245.
[8] Hashimoto T, Matsuzika K, Moses E, Onuki A. Phys Rev Lett 1995;74:126.
[9] Chopra D, Kontopoulou M, Vlassopoulos D, Hatzikiriakos SG. Rheol Acta 2002;41:10.
[10] Wolf BA. Macromolecules 1984;17:615.
[11] Horst R, Wolf BA. Macromolecules 1991;24:2236.
[12] Horst R, Wolf BA. Macromolecules 1992;25:5291.
[13] Horst R, Wolf BA. Macromolecules 1993;26:5676.
[14] Joanny JF, Leibler L. J Phys (Paris) 1978;39:951.
[15] Zinn-Justin J. Quantum field theory and critical phenomena. Oxford: Clarendon; 1989.
[16] Peterlin A, Turner DT. Polym Lett 1965;3:517.
[17] Laufer Z, Jalink HL, Staverman J. Polym Chem Ed 1973;11:3005.